Overlayers, interlayers, and surface alloys of Mn on the Cu(111) surface

G. Bihlmayer,* Ph. Kurz, and S. Blügel
Institut für Festkörperforschung, Forschungszentrum Jülich, D-52425 Jülich, Germany
(Received 26 January 2000)

The energetics of various surface alloys of manganese on copper (111) are calculated and their stability against clustering and/or interdiffusion is determined by an *ab initio* method. The interplay between stoichiometry, chemical, and magnetic ordering allows for a large variety of ordered alloys; only two are found to be stable against clustering: a 33% alloy and a 50% alloy of antiferromagnetically ordered Mn chains. Thermodynamic considerations indicate that only the 33% alloy will be formed at temperatures typical for epitaxial growth. The results are compared to recent scanning tunneling microscopy experiments.

I. INTRODUCTION

The study of magnetically stabilized surface alloys has attracted much experimental and theoretical interest in the past decade. Most work has been done on surface alloys on the (100) (Refs. 1–5) and (110) (Ref. 6) surfaces of Cu, Ag, and some transition metals. Of all investigated systems, the Mn/Cu surface alloy on the Cu(100) surface has attracted most attention: this surface alloy has been characterized with low-energy electron diffraction[1] (LEED) and scanning tunneling microscopy[2] (STM), and theoretical work[1] explained and confirmed these experimental results. No straightforward extension of the insights gained from these surfaces to the (111) surfaces of fcc crystals is possible: the close packing of the (111) layers will reduce the substantial relaxations observed in the more open surfaces and the triangular lattice formed by the hexagonal symmetry of the surface causes new possibilities of magnetic ordering of the atoms. This work provides a theoretical investigation of the possibility of the formation of a manganese surface alloy on the Cu(111) surface.

The stability of the (100) and (110) surface alloys was attributed to a magnetic effect in these alloys: the lower coordination and the missing nearest-neighbor magnetic atoms lead to an enhancement of the magnetic moment as well as to an outward relaxation of these atoms that reduces the coordination even more. The preferred magnetic ordering of Mn on an Ag(100) surface in an alloy as well as in a monolayer was found to be antiferromagnetic.[7,8] Therefore, we have to keep in mind the possibility of the formation of noncollinear structures on the hexagonal (111) surfaces. Alloys of high Mn content could form interesting combinations of magnetic and structural ordering.

An investigation of the growth of Mn on Ru(0001) (Ref. 9) and Ir(111) (Ref. 10) has shown that thin films of Mn grown epitaxially on these surfaces (as compared to thicker layers) have an enhanced magnetic moment. The ordering of these moments is unknown, but experiment shows that they are not coupled ferromagnetically. For thicker layers (more than four monolayers) Mn reconstructs to form close packed layers. The lattice constant of Ir is 6% larger than that of Cu, so we expect that Mn fits onto the Cu substrate. On the other hand, Tian *et al.*[11] reported on epitaxial Mn films grown on Pd(111) and found similar phases with a 6.3% larger lattice constant and a $(\sqrt{3}\times\sqrt{3})R30°$ superstructure on a Cu(111) substrate.[12] A recent STM study,[22] however, suggested that these phases were not pure Mn overlayers, but a Mn/Cu surface alloy. In this work it was shown that for submonolayer coverages near step edges a Mn/Cu alloy with an expanded in-plane lattice constant and a $(\sqrt{3}\times\sqrt{3})R30°$ structure is visible at the surface; in the subsurface layer an alloy of yet unknown structure was proposed. An experimental study of the (111) surfaces of Pt/Pt_3Mn layered systems[13] and a subsequent calculation[14] gave evidence for a magnetic alloy on the surface.

The aim of this work is the investigation of various Mn surface alloys on the Cu(111) surface, their magnetic structure, relaxations, and their stability. These alloys were selected such as to include all combinations of nearest-neighbor interactions in the basic triangle of the two-dimensional lattice. From earlier work on Mn surface alloys on Cu(100) (Ref. 3) and Ag(100) (Ref. 8) we expect that these interactions dominate the energetics of these alloys, and that the selected alloys are the most relevant ones. We do not include the investigation of a Mn bilayer nor a bilayer-alloy formation as this has not been observed so far for Mn/Cu(100) or Mn/Cu(110) and the number of possible magnetic and compositional configurations we would have to investigate to make definite predictions is very large. First steps in this direction have recently been made by Abt and Blügel[8] for Mn on Ag(100).

With total-energy calculations we probe the stability against cluster formation at the surface and against wetting by the substrate. In our studies we consider only the energy differences between alloy and wetted alloy or clustered surface, i.e., the kinetic and dynamic aspects of the formation of these states; the path and energy barriers of the exchange processes between the involved atoms are not captured. The paper is organized as follows: After a short description of the computational method we present the results for a Cu(111) surface with and without Mn overlayer and investigate the tendency for the Mn to diffuse into the bulk. We study the possibilities of alloy formation on the surface as well as in the deeper layers and conclude with a simple thermodynamical modeling of the disordered Mn/Cu surface alloy.

II. METHOD

We used the full potential linearized augmented plane wave method[15] (FLAPW) in thin film geometry as imple-

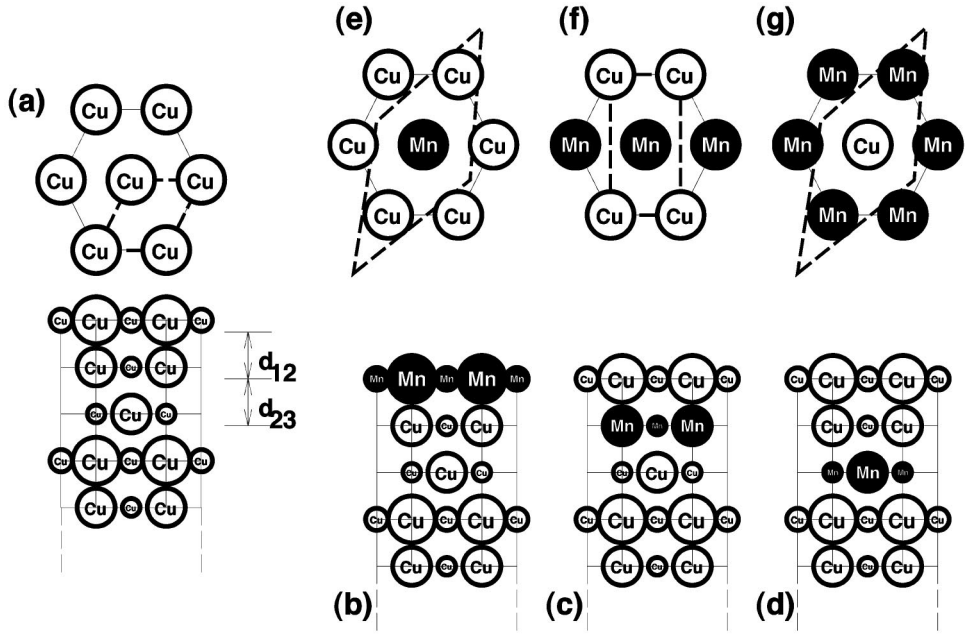

FIG. 1. Models of the clean (a) and the (one monolayer) Mn covered (b) Cu(111) surface and films with one monolayer Mn in the subsurface (c) and subsubsurface (d) layer. Alloys with 33%, 50%, and 66% Mn are shown in (e)–(g). Thick dashed lines indicate the two-dimensional unit cell, and d_{ij} is the interlayer distance between the layers i and j.

mented in the FLEUR program. Our calculation is based on the density functional theory in the generalized gradient approximation (GGA) as formulated by Perdew *et al.*[16] Using a scalar-relativistic Hamiltonian we employed a plane wave cutoff of $k_{\max}=4.0$ a.u.$^{-1}$ for the wave functions and $G_{\max}=13.5$ a.u.$^{-1}$ for the charge density. The muffin-tin radii were 2.18 a.u. for both Cu and Mn. The angular momentum expansion of the charge density inside the muffin-tin spheres was truncated at $l_{\max}=8$. For the $\mathbf{k}_{||}$-space integration, 45, 15, and 8 special $\mathbf{k}_{||}$ points were used in the irreducible wedge of the two-dimensional Brillouin zones of the unit cells containing 1, 2, and 3 surface atoms, respectively. A structure was considered relaxed when all the forces[17] on the atoms were smaller than 1 mhartree/a.u.

For our calculations we used nine layers of metal embedded in a semi-infinite vacuum to simulate the surface. For the lateral lattice constants we use the values obtained from a bulk calculation. We determined a lattice constant of $a_0^{\mathrm{Cu}}=6.83$ a.u., which is in very good ($+0.2\%$) agreement with the experimental value.

III. RESULTS

A. Surface segregation

1. Clean Cu(111) surface

As a first step we calculate the relaxation of a clean (uncovered) Cu(111) surface and compare these results with other data. We allow all layers to relax and minimize the forces exerted on the atoms. Compared with the ideal (bulk-truncated) interlayer spacing $d_{\mathrm{Cu(111)}}$, the first two Cu layers contract by $\Delta d_{12}=(d_{12}-d_{\mathrm{Cu(111)}})/d_{\mathrm{Cu(111)}}=-0.5\%$ [cf. Fig. 1(a)]. The second and third layers are also contracted by a tiny $\Delta d_{23}=-0.3\%$. Compared to the more open Cu(100) ($\Delta d_{12}=-4\%$) or the Cu(110) ($\Delta d_{12}=-8\%$), these relaxations are very small. An experimental study[18] of the Cu(111) surface reported a contraction of the first two layers of $\Delta d_{12}=-0.7\%$ and a calculation[19] within the local density approximation indicated a value of $\Delta d_{12}=-1.27\%$.

2. One ferromagnetic monolayer Mn on the surface and in the subsurface layers

To see if a (ferromagnetic) monolayer of Mn is stable on the Cu(111) surface or if Mn prefers to diffuse into the bulk or inner layers of the Cu substrate, i.e., Cu prefers to wet the Mn monolayer, we replaced the first, second, or third layer of the Cu film with Mn layers [Fig. 1(b)–(d)]. We denote these structures as CCCM (Mn in the surface layer) and CCMC and CMCC (Mn occupies the sub- and subsubsurface layer, respectively). Again, all layers were allowed to relax but no corrugation, reconstruction, or in-plane relaxation was permitted.

We compare the relaxations of the Mn layer systems with the uncovered, relaxed Cu(111) (denoted CCCC) and calculate the quantity $D_{ij}=(d_{ij}^{\mathrm{CCCM}}-d_{ij}^{\mathrm{CCCC}})/d_{ij}^{\mathrm{CCCC}}$ for the Mn overlayer and likewise for the buried Mn layers. From Table I we see that the Mn overlayer expands almost 5% outwards, and also the inner interlayer distances are affected by this expansion. This expansion is driven by the magnetism of the Mn overlayer, since a nonmagnetic calculation shows almost no differences in relaxation as compared to the uncovered Cu(111) surface. This expansion can also be seen in the surface alloys of the (111) surface (see below) and of the Cu(110)-$c(2\times2)$-Mn (Ref. 6) and Cu(100)-$c(2\times2)$-Mn (Ref. 1) surface alloys.

TABLE I. Changes in the relaxation (D_{ij}) of a Cu(111) surface with Mn in the surface (CCCM), subsurface (CCMC), and subsubsurface (CMCC) layer and the magnetic moment μ within the muffin-tin spheres of the Mn atoms in the structurally relaxed configurations.

	D_{12} (%)	D_{23} (%)	D_{34} (%)	D_{45} (%)	μ (units of μ_{B})
CCCM	4.89	2.15	1.91	1.11	3.15
CCMC	1.81	3.09	0.90	0.13	2.85
CMCC	0.78	2.84	2.99	1.15	2.60

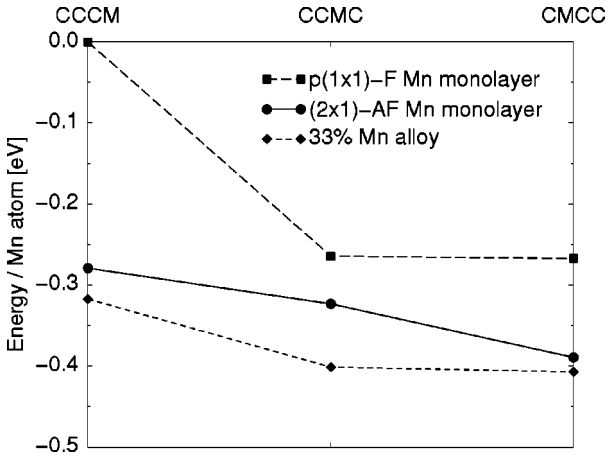

FIG. 2. Energy of several calculated magnetic and compositional configurations of Mn layers on and in Cu(111). The (2×1)-AF monolayer and the alloy are shifted with respect to the ferromagnetic CCCM structure by their respective stabilization energy. CCCM denotes a Mn covered Cu surface [Fig. 1(b)], while CCMC and CMCC indicate that Mn is in the subsurface [Fig. 1(c)] or subsubsurface layer [Fig. 1(d)], respectively.

In this calculation we assume that the magnetic ordering of the Mn atoms is ferromagnetic and with this restriction we find magnetic moments as indicated in Table I. When we compare the magnetic moment of the Mn overlayer on Cu(111) with the results of the (100) surface,[4] the more open (100) surface induces a higher moment of $3.45\mu_B$ compared to $3.05\mu_B$ for the (111) surface. Consequently, the moment of Mn decreases as it moves deeper into the bulk to $2.63\mu_B$ in the subsurface layer and $2.51\mu_B$ in the subsubsurface layer. From the total-energy calculation we see (Fig. 2) that Mn layers are also more stable when they are covered by Cu layers. This wetting energy $\Delta E_W = E_I - E_S$, defined as the difference between the energy of an interlayer (E_I) and an overlayer (E_S), is similar to the results for ferromagnetic Mn on the Cu(100) surface.[3]

3. Antiferromagnetic monolayers of Mn on the surface and in the subsurface layers

The magnetic structure of Mn on Cu(111) may be rather complicated. From previous calculations of Mn on Cu(100) (Ref. 3) we know that Mn favors the $c(2\times2)$ antiferromagnetic order. From this result we conclude that the nearest-neighbor exchange coupling between Mn atoms within a Mn monolayer will be antiferromagnetic (AF). An antiferromagnet on a triangular lattice, as provided by the (111) surface of Cu, is a prototypical example of a frustrated spin system. Frustration is the origin for a number of diverse phenomena such as noncollinear magnetism. Indeed the magnetic ground state of Mn on Cu(111) is unknown. The magnetic properties of these triangular antiferromagnets are typically described in terms of the classical Heisenberg model. Investigating the Heisenberg model with nearest, next-nearest, and next-next-nearest neighbor exchange coupling constants with respect to the possible magnetic ground-state structures, we found three commensurate magnetic phases to be considered: the ferromagnetic state with one atom per surface unit cell as discussed above, the columnar antiferromagnetic (2×1)-AF

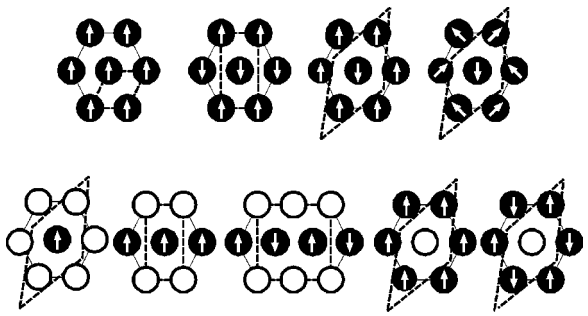

FIG. 3. Top: Four magnetic configurations of an Mn(111) layer: $p(1\times1)$-F, (2×1)-AF $(\sqrt{3}\times\sqrt{3})R30°$-AF, and $(\sqrt{3}\times\sqrt{3})R30°$-120°. Bottom: Magnetic and compositional configuration of the calculated ferromagnetic and antiferromagnetic surface alloys with 33%, 50% (F-chain and AF-chain structure), and 66% (66%-F, 66%-AF) Mn. The unit cells used in the actual calculation are indicated by thick dashed lines.

configuration with two atoms per unit cell, and the Néel state, a coplanar noncollinear $(\sqrt{3}\times\sqrt{3})R30°$-120° state with three atoms per unit cell. We included in addition a collinear $(\sqrt{3}\times\sqrt{3})R30°$-AF structure, which is a particular linear combination of the ferromagnetic and Néel state. The magnetic structures are shown in the top row of Fig. 3. From the total-energy calculations we find the rather surprising result that the columnar antiferromagnetic (2×1)-AF configuration is the most stable. Compared with the ferromagnetic solution it is stabilized by 0.28 eV per Mn atom and 0.04 eV more stable than the $(\sqrt{3}\times\sqrt{3})R30°$-AF ordering. Also, the noncollinear Néel structure, $(\sqrt{3}\times\sqrt{3})R30°$-120°, is almost 0.09 eV higher in energy than the columnar AF configuration.[20] This may suggest that an even more complicated spin structure will be the actual ground state,[21] and we have to keep in mind that our reference point of energy for the full monolayer coverage might still be a few meV too high.

Since the (2×1)-AF configuration is by far the most stable collinear magnetic state of a Mn overlayer on Cu(111), we now investigate the stability of this configuration against wetting. As we will discuss later for the alloys in more detail, the relaxations of the different magnetic structures are quite similar; the same is found for the overlayers. Thus, assuming no change of the relaxations when going from the ferro- to the antiferromagnetic over- and interlayers, we calculated the total energies of (2×1)-AF Mn in the second and third layers of Cu(111). The energies obtained by these calculations are shown in Fig. 2. We see, that in all layers this configuration is more stable than the ferromagnetic one, but the energetic differences are smaller in the deeper layers. From our calculations we derive that energetically the Mn monolayer is not stable at the surface. This supports the suggestion[22] that the interpretation of the LEED data of Mn on Cu(111) (Ref. 12) should be based on a more complex structural model. But the energy difference between the covered and uncovered Mn monolayer of 0.03 eV is small enough so that it could also be likely that a kinetic barrier stabilizes the Mn overlayer on the Cu(111) surface.

The magnetic moments of these (2×1)-AF configurations differ a little bit from than their ferromagnetic counterparts: the moments decrease from $3.15\mu_B$ at the surface to

TABLE II. Magnetic moment μ, relaxation of the Mn atoms ΔZ_{Mn}, relaxation of the first two layers Δd_{12}, and energy of formation per atom ΔE_F for ferromagnetic (F) and antiferromagnetic (AF) Mn/Cu alloys.

		μ (units of μ_{B})	ΔZ_{Mn} (a.u.)	Δd_{12} (%)	ΔE_F (meV)
33%	F	3.68	0.39	−0.4	−10
50%	F	3.53	0.29	−0.2	46
	AF	3.59	0.29[a]	−0.2[a]	−24
66%	F	3.55	0.25	+0.5	139
	AF	3.41	0.28	−1.2	29

[a]The relaxations for the 50% antiferromagnetic chain were taken from the ferromagnetic 50% alloy.

$2.82\mu_{\mathrm{B}}$ in the subsurface and $2.77\mu_{\mathrm{B}}$ in the subsubsurface layer.

B. Alloy formation

In the case of the (100) and the (110) Cu surfaces, the formation of a surface alloy was observed experimentally and theoretically. To investigate the possibilities of surface-alloy formation on the (111) surface, we calculate the ordered Mn/Cu layers depicted in Fig. 1(e)–(g), which include all structural combinations of nearest-neighbor interactions in the basic triangle of the two-dimensional lattice plus one additional configuration in order to independently check the validity of the nearest-neighbor approximation. Starting from these structural configurations we included all magnetic configurations as shown in Fig. 3 (bottom) with ferromagnetic and antiferromagnetic nearest-neigbor exchange interactions. As the magnetic interaction of the 33% alloy is a next-nearest-neighbor interaction, with tiny energy differences to the ferromagnetic configuration it is not important in the context of this work. Thus it is not subject to further investigations and has been ignored. Note that our total-energy calculations neglect the kinetic effects that may stabilize or prevent the formation of the alloy.

1. Ordered surface alloys

We define the formation energy of an alloy with x% Mn as $\Delta E_F = E^{\mathrm{alloy}} - [xE^{\mathrm{CCCM}} + (1-x)E^{\mathrm{CCCC}}]$, where all energies have to be taken per surface atom. Our sign convention is such that $\Delta E_F < 0$ means that alloy formation is energetically favored, while, if $\Delta E_F > 0$, phase separation is preferred. For E^{CCCM} we have to take the magnetic ground-state configuration, i.e., the antiferromagnetic overlayer. To eliminate the effects from differently sized unit cells, we calculated E^{CCCC} and ferromagnetic E^{CCCM} for a (2×1) and $(\sqrt{3}\times\sqrt{3})R30°$ cell and compared only energies of unit cells of the same size. The alloy atoms are allowed to relax perpendicular to the surface but again no in-plane relaxation was taken into account.

The magnetic moments, relaxations, and the formation energies of the configurations are listed in Table II. The 33% Mn alloy can be compared to the Mn/Cu(100) and (110) surface alloys, since there are no nearest-neighbor Mn-Mn interactions. Indeed, the outward relaxation (measured from the Cu position in the surface plane) of the Mn atom, ΔZ_{Mn}, of 0.39 a.u. is only 0.09 a.u. smaller than that for the Mn in the (100)-oriented 50% surface alloy and almost identical to the (110)-oriented one (0.38 a.u.). One has to be careful when comparing these results, since the latter two were obtained in the local density approximation (LDA). This may underestimate the relaxations, as it was shown to yield smaller magnetic moments.[4] In the GGA, the magnetic moment of the (100) surface alloy is $3.84\mu_{\mathrm{B}}$, while in LDA it is only 3.64. The LDA value for the (110) alloy is $3.82\mu_{\mathrm{B}}$ and our LDA calculation yields $3.51\mu_{\mathrm{B}}$ for the 33% (111) alloy so that the general rule, that magnetic moments in a close packed surface are smaller than on open ones is still conserved on the (111) surface.

The moments of the 50% and 66% alloys are smaller, since the numbers of nearest-neighbor (NN) Mn atoms are 2 and 3, respectively, and the Mn overlayer (6 NN Mn atoms) has an even smaller moment of $3.15\mu_{\mathrm{B}}$. Also the outward relaxation of the Mn atoms becomes smaller, which fits into the picture of the magnetovolume effect. As the Mn atoms move outward in the 33% and 50% alloys, the first two Cu layers resume almost the same distance as in the clean Cu(111) surface.

From the formation energies of Table II we see that the 33% alloy is stable against clustering and the value $\Delta E_F = -10$ meV indicates stability at lower temperatures. The ferromagnetic 50% (2×1) arrangement (F-chain structure) is already unstable against clustering and the ferromagnetic 66% $(\sqrt{3}\times\sqrt{3})R30°$ structure is highly unstable. But when we switch from this structure to the antiferromagnetic configuration we gain 110 meV. This large stabilization is not unexpected, since the energy difference between the ferro- and antiferromagnetic Mn overlayers was already 279 meV per Mn atom. There, four ferromagnetic NN Mn-Mn couplings were changed to antiferromagnetic coupling, while in the case of the 66% surface alloy only three bonds were changed.

This suggests that the F-chain alloy could gain up to 75 meV when the Mn chains couple antiferromagnetically, and this would be the most stable surface alloy. Indeed, we calculated this AF-chain structure and found a stabilization energy (as compared to the ferromagnetic alloy) of 70 meV, yielding a formation energy of −24 meV. Thus, the formation of this antiferromagnetic chain of Mn on a Cu (111) surface is, from an energetic point of view, highly favorable. Whether this alloy can be actually found on a surface depends, of course, on the kinetic barriers and entropic effects in the actual formation process.

One could speculate how an antiferromagnetic (or even noncollinear) arrangement of the Mn atoms in the 33% alloy would alter the stability of this alloy. But in this case, as the magnetic interaction is a next-nearest-neighbor interaction, we expect only tiny energy differences and did not investigate this configuration.

Along with the stabilization due to antiferromagnetic coupling of the Mn atoms we notice another interesting phenomenon. On the (100) and (110) surfaces it has been observed experimentally and theoretically that the formation of a $c(2\times2)$ Mn/Cu surface alloy causes a drop of the work function $\Delta\Phi$ as indicated in Fig. 4. We observe, that for a 50% Mn

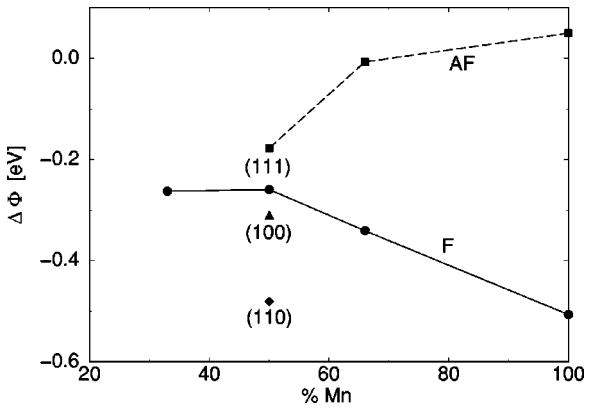

FIG. 4. Work-function changes $\Delta\Phi = \Phi^{\mathrm{Cu/Mn}} - \Phi^{\mathrm{Cu}}$ upon alloying of a Cu(111) surface with Mn. The solid line connects the ferromagnetic (F) structures, the dashed line the antiferromagnetic (AF) solutions. Results for the (100) (Ref. 1) and (110) surfaces (Ref. 6) are also indicated.

alloy the work-function change is smaller than in the previous two cases, but since the formation of a large magnetic moment should be responsible for this change, the smaller moment on the (111) surface results in a smaller effect.

Results for the 33% and 66% ferromagnetic alloys are also in line with this observation when we take into account that a smaller (larger) coverage leads to smaller (larger) effects. But the antiferromagnetic 66% Mn alloy shows almost no change of the work function and we see that the antiferromagnetic Mn overlayer has a work function even 50 meV higher than the Cu(111) surface.

While energetics and the work function are quite sensitive to the magnetic ordering, the magnetic moments and the relaxation are rather insensitive quantities in this respect. The magnetic moment of the antiferromagnetic 66% alloy is $0.1\mu_{\mathrm{B}}$ lower than that of the corresponding ferromagnetic alloy, and the outward relaxation of the Mn atoms 0.03 larger.

2. Subsurface alloys

In the last section we have shown that a 33% surface alloy in $\sqrt{3}\times\sqrt{3}$ arrangement and an antiferromagnetic 50% alloy in the (2×1) structure are stable against clustering on the Cu(111) surface. First, we will investigate the stability of the 33% alloy against interdiffusion into the bulk, since this resembles most closely the limiting case of the diffusion of an isolated atom into the bulk. The energetics of a single Mn atom in the sub- or subsubsurface layer is also important for the formation of other subsurface alloys. The stability of these alloys will be discussed at the end of this section.

As we did in the case of the Mn over- and interlayers, we substituted the subsurface and subsubsurface layer of the film with the Mn alloy and calculated the total energies of these arrangements. In this case we did not relax the structures, but used the interlayer distances as shown in Table I.

The energies obtained by this procedure are shown in Fig. 2. When a Mn atom moves from the surface to the subsurface layer, the energy gain is 84 meV, and when put into the subsubsurface layer the gain is almost 90 meV. The magnetic moment is reduced to $3.45\mu_{\mathrm{B}}$. This indicates that—although stable against clustering—the 33% alloy is not stable against wetting or interdiffusion into the bulk. Nevertheless we note that these interdiffusion energies are small and a stabilization of these surface alloys by kinetic barriers is probable. Also in the case of Mn alloys on Cu(100) surfaces a small negative wetting energy was found; nevertheless these alloys can be observed in experiment.

We also calculated the stability of the 50% alloys against interdiffusion. For the AF-chain structure an energy of 63 meV per Mn atom is gained when the Mn atoms are in subsurface positions. Interestingly, for the same ferromagnetic alloy this energy amounts to 99 meV per manganese atom. Here, we observe the same trends as those for the full Mn monolayers, where also the antiferromagnetic monolayer was far more stable against wetting than the ferromagnetically ordered one.

3. Disordered surface alloys

In recent STM experiments[22] at 320 K it was found that at kinks, single Mn atoms are incorporated in the Cu(111) substrate and form a seam of a Mn/Cu alloy near the step edge. In the initial stage of growth, isolated Mn atoms were observed in the substrate that formed a two-layer alloy at higher coverages whose composition in the subsurface layer could not be detected. The surface layer showed clear indication of a Mn/Cu alloy with a $(\sqrt{3}\times\sqrt{3})R30°$ structure compatible with a 33% alloy. The in-plane lattice constant was expanded by 9.4% with respect to the Cu surface and exhibited an additional dislocation network with a larger periodicity.

For a better understanding of the initial stages of alloy formation a qualitative description of the Cu-rich side of the phase diagram of the disordered surface alloy would be desirable. To this end, we employ a very crude cluster variation method[23] to get an idea of the miscibility gaps in the phase diagram of the two-dimensional surface alloy. Employing the natural iteration method for a ternary alloy[24] we treat the two magnetically inequivalent Mn atoms as different species, keeping in mind that the actual, binary phase diagram of the Mn/Cu surface alloy is only a cut through this ternary diagram, where the ratio of spin-up to spin-down Mn atoms minimizes the free energy.

Ignoring the Cu substrate and considering only the topmost layer containing the Mn/Cu alloy we can decompose this Mn/Cu surface lattice into triangles ijk, where the indices ijk indicate whether a Cu or a Mn atom (with spin up or down) can be found on the three corners of the triangle. Then, in a very simplified model, it is possible to associate energies ϵ_{ijk} with these triangles, so that the total energies E_{tot} of the different ordered surfaces can be written as sum of these energies: $E_{\mathrm{tot}} = \Sigma w_{ijk}\epsilon_{ijk}$. The weights or cluster probabilities w_{ijk} give the number of triangles (ijk) that can be found for the surface alloy with the energy E_{tot}. Since these weights are different on surfaces with different stoichiometry and/or magnetic order, knowing a set of E_{tot}, we can calculate the ϵ_{ijk}.

The same procedure can be applied to our films that include, in addition to the surface alloy, some layers of Cu(111) substrate. We still can use the total energies E_{tot} from different surface alloys, but we have to use the unrelaxed structures to make the decomposition in the ϵ_{ijk}'s. With these energies, we can try to predict the energies of other ordered and disordered surface alloys.

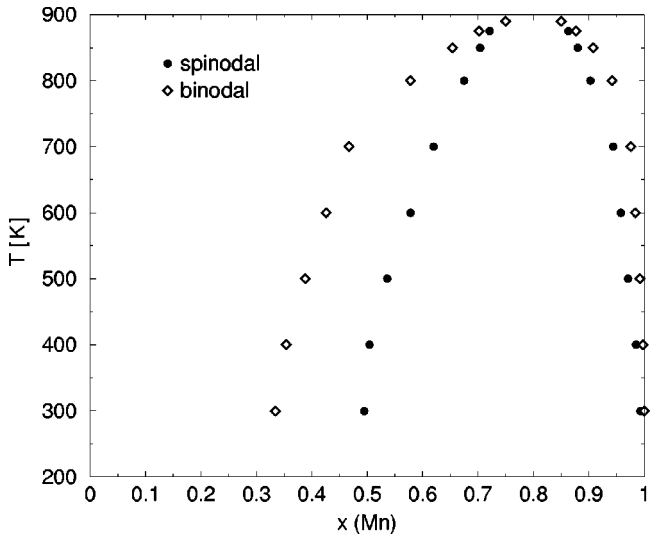

FIG. 5. Phase diagram for the disordered Mn/Cu(111) surface alloy obtained by triangle cluster approximation. The binodal line is indicated by open diamonds, and the spinodal curve by full circles. The ratio of Mn atoms with up or down spins is 1:1.

We can identify six different configurations that can be extracted from the eight collinear structures shown in Fig. 3: triangles that contain 0, 1, 2, and 3 atoms of Mn, the latter two with two different magnetic states. As a test we can try to calculate the energy of the 50% alloy from the 33% and 66% alloys and predict an energy that is 13 meV per surface atom off the self-consistently calculated value. From this difference we conclude that the error of the triangle approximation is in the range of relaxation energies that cannot be included in the formalism. This also suggests that we can only expect a qualitative description of the phase diagram.

In Fig. 5 we plot the phase diagram for the Mn/Cu(111) surface alloy. The minimal free energy was always found for an alloy with an equal amount of spin-up and spin-down Mn atoms. At the experimentally relevant temperatures the disordered phase is stable up to a Mn concentration of approximately 33%. If we define an order parameter η_1 as the sum over all cluster probabilities where the cluster contains two Cu and one Mn atom, we find that at this concentration $\eta_1(273\ \mathrm{K})=0.66$. With falling temperature η_1 increases to reach a value close to unity. This corresponds to the ordered $(\sqrt{3}\times\sqrt{3})R30°$ arrangement of the 33% Mn surface alloy. Defining η_2 as the sum over all cluster probabilities where the cluster contains one Cu atom and two Mn atoms of opposite spin, we can characterize the ordered antiferromagnetic 50% alloy by $\eta_1=\eta_2=0.5$. The 50% alloy—although metastable at temperatures above 300 K—shows no tendency to order as an antiferromagnetic chain structure. These results are consistent with the experimental observations of the initial stages of alloy formation, where locally only an ordered 33% Mn surface alloy with $(\sqrt{3}\times\sqrt{3})R30°$ structure was found.

IV. SUMMARY

In this paper we investigated the possibilities of surface-alloy formation for Mn on a Cu(111) surface. Neglecting any temperature and kinetic effects we found that an ordered 33% alloy with a $(\sqrt{3}\times\sqrt{3})R30°$ structure and a 50% alloy forming antiferromagnetic chains are stable against clustering at the surface. Thermodynamic considerations indicate that the 50% alloy will not be formed at temperatures typical for epitaxial growth. Both alloys and the Mn overlayer are unstable against wetting by Cu, but the wetting energies are small. This indicates that—depending on the actual conditions of growth—such surface alloys or, as seen in STM experiments,[22] more complex bilayer alloys can be formed. The theoretical and experimental investigation of these structures leaves plenty of room for future investigations.

ACKNOWLEDGMENTS

The authors gratefully acknowledge support from the TMR network Contract Nos. EMRX-CT96-0089 and FMRX-CT-0178 and from the Deutsche Forschungsgemeinschaft Grant BL444/1-1. One of us (G.B.) thanks the Center for Materials Science (CMS) for use of computing facilities.

*Electronic address: G.Bihlmayer@fz-juelich.de

[1] M. Wuttig, Y. Gauthier, and S. Blügel, Phys. Rev. Lett. **70**, 3619 (1993).
[2] M. Wuttig, S. Junghans, T. Flores, and S. Blügel, Phys. Rev. B **53**, 7551 (1996).
[3] S. Blügel, Appl. Phys. A: Mater. Sci. Process. **63**, 595 (1996).
[4] T. Asada and S. Blügel, Physica B **237-238**, 359 (1997).
[5] O. Rader, W. Gudat, C. Carbone, E. Vescovo, S. Blügel, R. Kläsges, W. Eberhardt, M. Wuttig, J. Redinger, and F.J. Himpsel, Phys. Rev. B **55**, 5404 (1997).
[6] Ch. Ross, B. Schirmer, M. Wuttig, Y. Gauthier, G. Bihlmayer, and S. Blügel, Phys. Rev. B **57**, 2607 (1998).
[7] S.C. Hong, M. Kim, and A.J. Freeman, J. Appl. Phys. **83**, 7016 (1998).
[8] R. Abt and S. Blügel, Philos. Mag. B **78**, 659 (1998).
[9] A.S. Arrot, B. Heinrich, S.T. Purcell, J.F. Cochran, and K.B. Urquhart, J. Appl. Phys. **61**, 3721 (1987).
[10] W.L. O'Brien and B.P. Tonner, J. Vac. Sci. Technol. A **13**, 1544 (1995).
[11] D. Tian, H. Li, S.C. Wu, F. Jona, and P.M. Marcus, Phys. Rev. B **45**, 3749 (1992).
[12] D. Tian, A.M. Begley, and F. Jona, Surf. Sci. Lett. **273**, L393 (1992).
[13] S. Gallego, C. Ocal, M.C. Muñoz, and F. Soria, Phys. Rev. B **56**, 12 139 (1997).
[14] S. Gallego, L. Chico, and M.C. Muñoz, Phys. Rev. B **57**, 4863 (1998).
[15] E. Wimmer, H. Krakauer, M. Weinert, and A.J. Freeman, Phys. Rev. B **24**, 864 (1981); M. Weinert, E. Wimmer, and A.J. Freeman, *ibid.* **26**, 4571 (1982).
[16] J.P. Perdew, J.A. Chevary, S.H. Vosko, K.A. Jackson, M.R. Pederson, D.J. Singh, and C. Fiolhais, Phys. Rev. B **46**, 6671 (1992).
[17] R. Yu, D. Singh, and H. Krakauer, Phys. Rev. B **43**, 6411 (1991).
[18] S.Å. Lindgren, L. Walldén, J. Rundgren, and P. Westrin, Phys. Rev. B **29**, 576 (1984).
[19] Th. Rodach, K.-P. Bohnen, and K.M. Ho, Surf. Sci. **286**, 66 (1993).

[20] Ph. Kurz, G. Bihlmayer, and S. Blügel, J. Appl. Phys. **87**, 6101 (2000).
[21] Ph. Kurz, K. Hirai, and S. Blügel (unpublished).
[22] J. Schneider, A. Rosenhahn, and K. Wandelt, Appl. Surf. Sci. **142**, 68 (1999).
[23] R. Kiguchi, Phys. Rev. **81**, 988 (1951).
[24] R. Kiguchi, Acta Metall. **25**, 195 (1976).